COMPARISON OF THE PERFORMANCE OBTAINED IN A TROPICAL COUNTRY, OF A SOLID ADSORPTION, SOLAR-DRIVEN REFRIGERATOR AND A PHOTOVOLTAIC REFRIGERATOR

A. ADELL

Laboratoire de Physique Atmosphérique, Faculté des Sciences, 04 BP 322 Abidjan 04 (Ivory Coast)*

(Received July 12, 1984; in revised form September 25, 1984)

Résumé

Il a été réalisé un prototype de réfrigération solaire à adsorption solide (zéolithe 13 x–eau) qui a été testé sous un vrai soleil, dans les conditions climatiques d'Abidjan (climat équatorial). Simultanément un réfrigérateur photovoltaïque du commerce a été testé dans des conditions d'utilisation semblables. Les performances d'ensemble des deux appareils ont montré un léger avantage pour le réfrigérateur photovoltaïque. Un bilan très détaillé basé sur l'analyse des irréversibilités de fonctionnement, a été fait. Il doit permettre de traiter les problèmes d'optimisation thermodynamique et économique de ce genre d'appareil, d'une façon complète.

Summary

A prototype solid adsorption solar refrigerator has been constructed (zeolite 13 x–water) and tested in the sun under the equatorial weather conditions of Abidjan. A commercial photovoltaic refrigerator was simultaneously tested under similar conditions. The solar coefficient of performance of these two plants was slightly better for the photovoltaic refrigerator. A detailed evaluation using irreversibilities analysis, which allows total optimization of thermodynamic and economic problems has been made.

1. Introduction

An important part of the world's energy resources is utilized to produce low temperatures, especially in tropical countries such as the Ivory Coast, where it consumes 45% of the national electricity production. The possibil-

*On leave at: Laboratoire de Chimie-physique, Université des Sciences et Techniques, Place E. Bataillon, 34000 Montpellier, France.

0378-7753/85/$3.30

ity of solar driven refrigeration has been the subject of numerous researches, but to date the paucity of industrial applications is evidence of the difficulties encountered. Among the difficulties specific to the production of low temperatures (by comparison with the production of heat) by solar irradiation, are:

(a) energy saving is not large;
(b) the cost of the equipment is greater;
(c) the chilling ability of all solar refrigerating systems is low;
(d) the complementary supporting systems are expensive;
(e) technical problems are complex.

Of the various means of producing low temperatures using solar energy, the employment of the solid adsorption intermittent cycle is comparatively little known [1]. Nevertheless, this system offers many advantages over other, more developed, systems, namely:

(a) simplicity of operation (no moving parts);
(b) total autonomy (no requirement for electricity and water);
(c) low cost of operation and maintenance.

The system, which requires little sophisticated technology, is appropriate to the developing countries: the three stages essential when commercialising a product — conception and research, manufacture of elements, and installation and maintenance — can today be carried out entirely within the developing countries. In contrast to liquid absorption systems which satisfy a need for lower temperatures in summer and for heat in winter *via* their hot primary circuits, the solid adsorption system provides a direct answer to the low temperature requirements specific to hot countries. It also furnishes a means of preserving agricultural products of tropical origin in warehouses, which require rather high storage temperatures (up to 8 °C) [2].

The aim of this work was to carry out a detailed comparison of the performance of a solid adsorption solar refrigerator prototype with that of a commercial photovoltaic refrigerator.

2. Graphical exergetic analysis

Graphical exergetic analysis is a well-known method of studying the refrigeration process [3], and we have used it to study the intermittent solid adsorption cycle [4]. We now propose to use it to study the performance of the two types of refrigerator.

For a fluid flow, the exergy of the unit mass of fluid is:

$$\mathrm{ex} = h - h_0 - T_0(s - s_0) \tag{1}$$

where h and s are the specific enthalpy and entropy, respectively, and the subscript 0 refers to a standard state called the "dead state". For a refrigerating fluid, the dead state is the liquid phase at the temperature and pressure (T_0P_0) of the surroundings. The last term in eqn. (1) is called anergy:

$$\mathrm{an} = T_0(s - s_0) \tag{2}$$

The second law of thermodynamics may be rewritten as:

$$\frac{dm_1}{dt} ex_1 - \frac{dm_2}{dt} ex_2 + \frac{dq}{dt}\left(1 - \frac{T_0}{T_{sink}}\right) + \frac{d\tau_m}{dt} - T_0\left(\frac{ds}{dt}\right)_{universe} = 0 \quad (3)$$

where dm_1/dt and dm_2/dt represent the flow of matter entering and leaving the system, dq/dt is the heat flow provided by a reservoir at a temperature of T_{sink}, $d\tau_m/dt$ is the mechanical power input to the system, and $(ds/dt)_{universe}$ is the irreversibility power of the system. The exergy represents the maximum work (availability) that the flow of unit mass of fluid is able to give to the exterior when flowing into the dead state. This maximum work takes place when all the processes acting on the system are reversible. Assuming that heat rejection in the condenser of the refrigerator occurs at the temperature of reference, T_0, the use of eqn. (3) for the unit mass of fluid in permanent flow within a compressor refrigerator cycle leads to:

$$\text{necessary exergy } (\tau_m) = \text{desired exergy } \left(Q_{int}\left(1 - \frac{T_0}{T_{int}}\right)\right) + \text{exergy losses} \quad (4)$$

where the subscript "int" refers to the interior of the refrigerating compartment. Exergetic losses may be evaluated graphically from the entropy chart, in conformity with eqn. (1), using the equation:

$$dh = dex + dan \quad (5)$$

3. Results

3.1. Meteorological data

Solar global irradiation of 1 m^2 of collector (E): 20.5×10^6 J/day
Normal temperature (T_0): 29 °C
Nocturnal adsorption temperature (T_{night}): 26 °C
Mean wind speed: 2 m/s
Nebulosity: 20%.

3.2. Photovoltaic refrigerator

Electrical supply

An electronic regulation system assures protection of the batteries.
Mean energetic efficiency of the cells (η^{en}_{cell}): 0.12
Area coefficient ($coef_{area}$): 0.75
Energetic restitution coefficient of the batteries ($coef_{rest}$): 0.70

Compression system

The compression system is of the hermetic type, and includes a direct current electric motor with a fixed induction armature supplied from batteries by an electronic commutation unit and a piston compressor with a precooler.

— Electric motor:
  nominal voltage (V): 24
  internal resistance (r): 2.7 Ω
— Compressor:
  refrigerating fluid: R 12
  mean mechanical efficiency (η_{mech}): 0.80
  cubic capacity (displacement volume of the piston, simple effect): 2.61 cm^3
  clearance volume: 0.093 cm^3
  quality factor of polytropic compression (ρ): 0.10
  polytropic efficiency ($\eta_p = 1 - \rho$): 0.90

Heat transfer equipment
Overall heat transfer coefficient of condenser $(h.t.c.)_c$: 12 W/°C
Overall heat transfer coefficient of evaporator $(h.t.c.)_e$: 7 W/°C
Overall heat transfer coefficient of refrigerating compartment $(h.t.c.)_b$: 2 W/°C

Utilization mode

The photovoltaic refrigerator used was of the domestic type, with a refrigerating compartment capacity of 160 l, and an insulation thickness of 10 cm. The thermal regulation of the system used a hit or miss governor, in which the compressor undergoes a succession of working and non-working periods governed by a thermostat located in the refrigerating compartment. Discounting the *transient phases* which occur when opening the door and loading the refrigerator, the refrigerator functions with an *established regime*; this is characterized by variable working conditions that recur periodically, and during which the physical parameters change appreciably. Because the duration of the cycle of the refrigerating fluid in the compressor is fast compared with the variation of the parameters of the regime, one can estimate that the fluid undergoes a *quasi-permanent type flow* and apply the results for permanent flow to the analysis of the characteristics of this cycle.

The utilization mode of the refrigerator is determined by the thermostat position (degree of chill), the load coefficient (quantity and nature of the chilled products), and ambient conditions. This utilization mode corresponds to a minimal (optimum) collector area (S_{min}) necessary for the collection of solar irradiation. For a given utilization mode, the relatively restricted amplitude of temperature variation at different points in the cycle (15 °C at the evaporator, for instance), allows the mode to be characterised for cold production by a constant mean working regime: the average is taken over the working period of the compressor and leads to the steady state operating conditions.

3.3. Solid adsorption refrigerator

In the solid adsorption refrigerator the refrigerant (water) is adsorbed during the night by a molecular sieve (granular zeolite 13 x) reducing the temperature of the evaporator. During the day, solar irradiation, collected directly at the zeolite level, causes water desorption which assumes liquid phase in the condenser. The thermodynamic behaviour of the adsorption couple is adequately described by the semi-empirical equation of Dubinin (see ref. 1):

$$m = m_0 \exp\left[-A\left(\frac{T - T_c}{T_c}\right)^2\right] \tag{6}$$

where m is the mass of water adsorbed at temperature T and at the pressure of saturated vapor at T_c, m_0 is the maximum mass of water adsorbable, and A is a constant characteristic of the couple (A = 4.33 M.K.S., m_0 = 0.269 kg/kg of anhydrous zeolite).

The solar collector used was of the flat-plate type; it contained 13 kg of anhydrous zeolite, its area was 0.5 m^2, its absorbent surface was covered by a selective layer of black chrome and its back insulation consisted of 8 cm of glass wool. The collector had a single glass cover and its total heat capacity (c) was: 3×10^4 J/°C. Our prototype was not automated, and the valves had to be activated manually each morning and evening. The solid adsorption refrigerator functions essentially with a variable and intermittent regime. It is, however, possible to represent its operation by a set of cycles that undergoes a continuous permanent flow by breaking down the daily mass of cycled water (m) into a sufficient number of small, equal portions, Δm.

This method of breakdown into portions may also be used for compression systems, but the additional precision so obtained is less justified on account of the lesser variation of the regimes.

4. Experimental entropy charts

The two refrigerators were tested under approximately similar conditions, in order that a practical comparison could be made. In particular, the mean temperature of the evaporator of the photovoltaic refrigerator, $\overline{T}_{ev}$ (where the bar indicates that the average of the working period of the motor is taken), was taken as being equal to 0 °C, the same as the evaporation temperature of the solid adsorption refrigerator, fixed at 0 °C to allow cold storage in ice form. The value $\overline{T}_{ev}$ = 0 °C, for the photovoltaic refrigerator was obtained with the thermostat set in a position for $\overline{\overline{T}}_{int}$ equal to 8 °C (where the two bars over the interior temperature of the refrigerating compartment indicate that the average is taken over the total working and non-working periods during the regime established), which corresponded with a $\overline{T}_{ev}$ of 2 °C.

Photovoltaic refrigerator

The experimental temperature noted at the different points of the compressor cycle (1, 2, 3, 4′, 5, 6 and 7), allowed the entropy chart of 1 kg of the refrigerant R 12 to be drawn (Fig. 1). The path 3 - 4′, which corresponded to the actual polytropic compression, was replaced by the isentropic path 3 - 4 in the cycle efficiency calculation, to take account of the indicated efficiency of the compressor, which here is related to the operation of a perfect compressor, that is, an isentropic compressor without clearance volume (note that the volumetric efficiency, η_v, which is taken as approximately equal to the indicated efficiency, is calculated from actual conditions at the discharge point, 4′). From Fig. 1 one obtains the following data: exergetic efficiency of the cycle — including evaporator losses — (η^{ex} cycle) = 0.34; energetic efficiency of the cycle (η^{en} cycle) = 4.57; indicated efficiency ≃ volumetric efficiency ($\eta_{ind} \simeq \eta_{vol}$) = 0.87; electrical current in the armature (I) = 3.83 A; motor f.c.e.m. (E') = 13.6 V; electrical efficiency of the motor (η_{el}) = 0.57; rotary speed (N): 1890 rotations/min; electrical power (P_{el}) = 92 W; frigorific power = ($\rho_f = \rho_{el} \times \eta_{el} \times \eta_{mech} \times \eta_{ind} \times \eta^{en}_{cycle}$) = 166.5 W; mean isentropic expansion coefficient (γ) = 1.046; mean polytropic expansion coefficient (m) = 1.053; flow rate of refrigerant (D) = 4.85 kg/h.

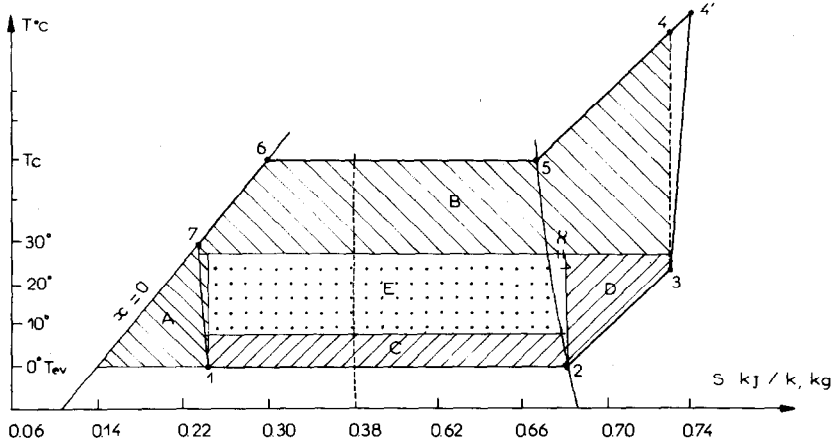

Fig. 1. Entropic chart for 1 kg of refrigerant R 12. The exergetic losses of each element are represented by the hatched surfaces. A, throttling device; B, condenser; C, evaporator; D, overheating suction; E, desired exergy (dotted surface).

Solid adsorption refrigerator

The total mass of cycled water was 340 g, which we considered in 5 equal portions, $\overline{\Delta m}$ = 68 g. The temperature of the different points of the entropic chart were calculated for the 5 cycles of the 5 portions according to eqn. (6), assuming that the enthalpy of water adsorption by zeolite is constant ($\Delta h_{ads} = 3.25 \times 10^6$ J/kg). The mean condensation temperature was 52 °C, and the nocturnal temperature 26 °C.

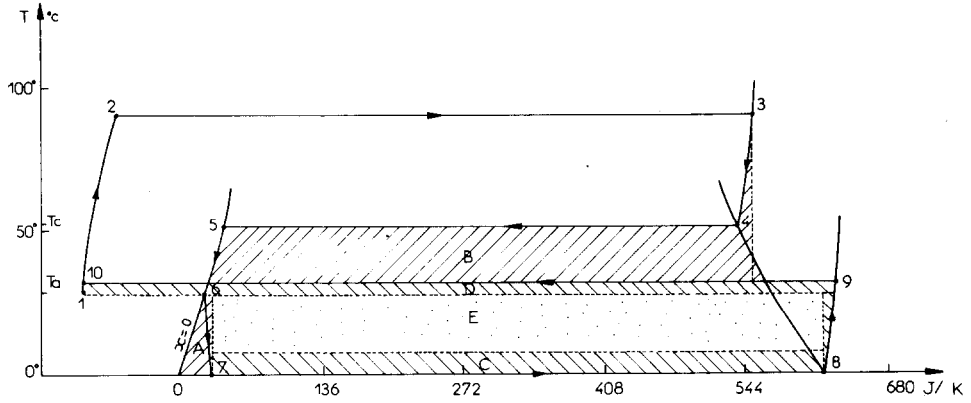

Fig. 2. Entropic chart of the first cycle corresponding to the desorption of 68 g of water (first portion). The different paths of the water cycle are: 1 - 2, isosteric heating of adsorbed water; 2 - 3, isothermal and isobaric desorption; 3 - 4, isobaric desuperheating of vapor; 4 - 5, isothermal and isobaric condensation; 5 - 6, cooling in accumulating bottle; 6 - 7, expansion into the evaporator; 7 - 8, isothermal and isobaric evaporation; 8 - 9, isobaric heating; 9 - 10, isothermal and isobaric adsorption; 10 - 1, isosteric return to nocturnal surrounding temperature. The exergetic losses corresponding to the different elements of the plant are represented by the hatched surfaces: A, Throttling device, B, condenser; C, evaporator; D, adsorption losses; E, desired exergy (dotted surface).

The exergy of sensible heat was calculated from the formula:

$$\text{EX. sens. heat} = C(T_{max} - T_0) - CT_0 \ln(T_{max}/T_0) = 0.38 \times 10^6 \text{ J} \quad (7)$$

where C is the total heat capacity of the empty collector plus the heat capacity of the anhydrous zeolite plus the heat capacity of residual water that has not been cycled. T_{max} is the maximum temperature attained by the collector during desorption (T_{max} = 398 K).

The preceding results were obtained using the total mass of water cycled and the daily solar irradiation as the only experimental data. It is possible to make a more accurate analysis if other experimental data such as the solar irradiation graph for a day, T_{cond} or T_{ev} temperature changes, pressure losses in the pipes, etc., are available. This detailed analysis is the essential objective of the exergetic method which attempts to make the best use of all the available data. If one possesses the solar irradiation graph as a function of time, for instance, it is then possible to obtain the detail of the losses of the collector (optical losses, losses coming from the irreversibilities of visible radiation absorption, losses of thermal radiation and convection at the surface). This more detailed analysis has already been presented in ref. 4.

5. General results

The different daily exergetic flows for the two refrigerators are given for a collection area of 1 m^2. A security coefficient ($coef_{secu}$ = 0.80), which

reduces the effect of the variability of solar irradiation by the storage of 20% of the daily received energy, has been taken for each plant. The load coefficient ($coef_{load}$), which represents the ratio of the reduction in temperature produced during the transient phase of opening the door and loading the refrigerator to the total reduction in temperature due to the plant, has been taken as being equal to 1/3. This corresponded to the refrigeration of about 20 kg of water every day by the photovoltaic refrigerator under the conditions of use.

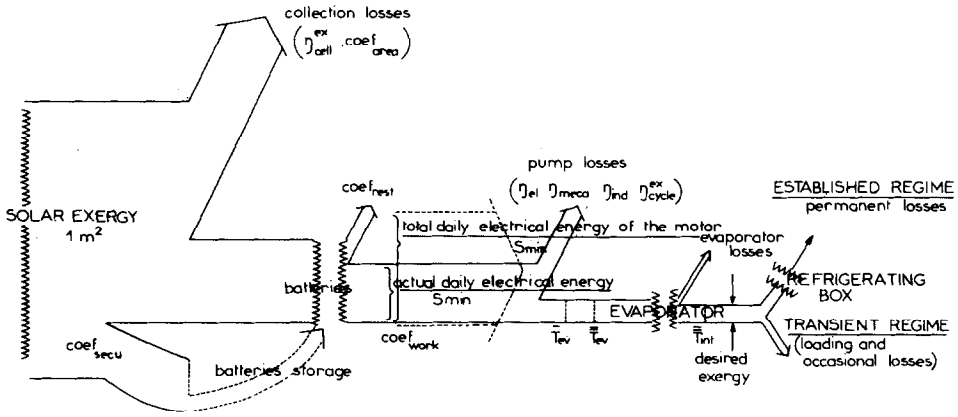

Fig. 3. Diagram of the principal exergetic flows in the photovoltaic refrigerator.

Figure 3 shows the principal exergetic flows in the photovoltaic refrigerator, and for the steady state operating conditions, one can write:

energy balance

$$S_{min} \times E \times coef_{secu} \times \eta_{cel}^{en} \times coef_{area} \times coef_{rest} \times \eta_{el} \times \eta_{mech} \times \eta_{ind} \times \eta_{cycle}^{en} \times \times (1 - coef_{load}) = (h.t.c.)_b \times (T_0 - \bar{T}_{int})$$

exergy balance

$$S_{min} \times E \times \left(1 - \frac{T_0}{T_s}\right) \times coef_{secu} \times \eta_{cel}^{ex} \times coef_{area} \times coef_{rest} \times \eta_{el} \times \eta_{mech} \times \times \eta_{ind} \times \eta_{cycle}^{ex} \times (1 - coef_{load}) = (h.t.c.)_b \times (T_0 - T_{int}) \times \left(\frac{T_0}{\bar{T}_{int}} - 1\right)$$

where T_s is the sun radiation temperature.

From this one can find the minimum collector area necessary for the utilization mode presented: $S_{min} = 2.9$ m^2. This refrigerator is sold with a collection area equal to 3.9 m^2 for use in a mode more demanding than that which we studied, and also with a daily mean solar irradiation lower than that of the day on which measurements were carried out. It must be noted that the supplementary energy so collected was in our application, stored in the batteries. If one defines the working coefficient ($coef_{work}$) of the motor as the ratio of the duration of the working period of the motor to the total

duration of working and non-working periods, the total working coefficient is found to be 0.38, and the working coefficient during the established regime is only 0.25. These relatively low values correspond well with the sub-utilization of the capabilities of this refrigerator, the compression group of which is intended for nominal use at 2500 r.p.m., an electrical efficiency of 0.75, and a mean evaporator temperature of −25 °C.

Figure 4 shows the principal exergetic flows in the solid adsorption refrigerator. Because the collector surface (0.5 m^2) of the prototype used could not be modified, the heat transfer coefficients of evaporator and refrigerating compartment were adjusted to obtain a similar T_{int} for the two plants.

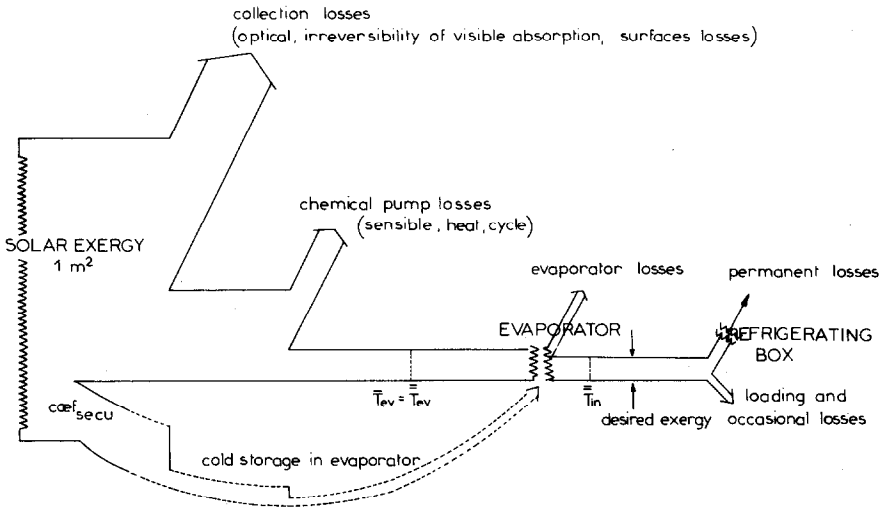

Fig. 4. Diagram of the principal exergetic flows in the solid adsorption refrigerator.

Table 1 lists the results obtained for the two types of refrigerator using a 1 m^2 collector.

6. Discussion and conclusion

The detailed analysis carried out on the two solar refrigerating systems may be used for an all embracing study of optimum thermodynamic and economic design. This type of analysis will become more and more useful when studying commercial projects, because of two vital factors: first, all solar refrigerating systems have insufficient frigorific capacity per unit area of collector to satisfy certain needs such as air conditioning, where the collector surface is almost always limited to the roof, and where roof area requirements in wet tropical countries are more than twice the area available on present warehouses. Secondly, the economic competitiveness of solar driven refrigerating plants is very uncertain at the present time, and is more

TABLE 1

Results for 1 m^2 collector — 10^6 Joules

	Daily solar irradiation	Daily solar exergy	Stored exergy	Collection losses			Pump losses			Losses resulting from the irreversibilities in the cycle (including evaporator losses)				Exergy given to the refrigerating compartment	Solar exergy efficiency (%)	Solar cop (%)
Photovoltaic refrigerator	20.52	19.47	3.89	Cell efficiency	$Coef_{area}$	$Coef_{rest}$	Electrical efficiency	Mechanical efficiency	Indicated efficiency	Throttling	Condenser	Evaporator	Overheating suction	0.14	0.71	9.0
				13.61	0.49	0.44	0.45	0.12	0.06	0.01	0.18	0.07	0.01			
				Total = 14.54			Total = 0.63			Total = 0.27						
Solid adsorption refrigerator	20.52	19.47	3.89	Visible absorption irrevers-ibilities	Optical losses	Surface losses	Sensible heat			Throttling	Condenser	Evaporator	Adsorption losses	0.12	0.61	7.8
				10.40	3.68	0.48	0.67			0.01	0.09	0.04	0.09			
				Total = 14.56			Total = 0.67			Total = 0.23						

difficult to achieve than for devices producing heat by means of solar energy. It should be noted that, using the same collector area, ten times less electricity is saved in reducing temperatures than is used in raising temperatures. Furthermore, the cost of solar refrigerators is very high: a photovoltaïc refrigerator costs (selling price) more than ten times that of an equivalent electrical or petroleum operating refrigerator.

A comparison of the experimental operation of the two plants, as they have been presented (that is, unoptimized), has shown that the daily cold production per unit area of collector, is about the same (slightly more in the case of the photovoltaic refrigerator). Details of the exergetic losses also show similar behaviour for all the different phases of cold production.

In spite of the many advantages presented in the Introduction, detailed analyses of the operation of solid adsorption refrigerators have revealed some disadvantages that make their use less convenient than photovoltaic refrigerators:

(a) such refrigerators are without a thermal regulation system; this restricts the use of a particular plant to a very small field and makes mass production of the refrigerators more difficult;

(b) energy storage presents a serious problem; a satisfactory economical solution has not yet been found. It may be solved by employing chemical elements (such as eutectic salt solutions), having a suitable freezing point, in an evaporator with a double partition. This storage in latent heat form would also have the advantage of reducing the amplitude of temperature variation at the chilled load level and protect against any deterioration in performance resulting from a too low evaporation temperature during nocturnal adsorption. When water is used as a refrigerant, the cold storage can take place in ice form directly in the evaporator but this limits the evaporator temperature to 0 °C;

(c) automatic operation of this type of plant, which is easily accomplished using static pressure valves, must be combined with an optimized complex electronic system;

(d) the collector performance of this type of plant depends on the environmental conditions (ambient temperature, wind, etc.). These reinforce the variable character of daily temperature reductions resulting from the solar irradiation variability.

It must be pointed out that, from a reliability aspect, the solid adsorption refrigerator, which was tested for a period of one year, gave problems in maintaining a vacuum, whereas the photovoltaic refrigerator failed at the electronic unit level.

List of symbols

The principal symbols for the solid adsorption refrigerator have been used previously in ref. 4.

η_{en} Energetic efficiency

η_{ex} Exergetic efficiency: required exergy/necessary exergy

η_{el} Electrical efficiency of the motor

η_{mech} Mechanical efficiency of the compressor

η_{ind} Indicated efficiency of the compressor as given by Watt's indicator

η_{vol} Volumetric efficiency: ratio of the new volume of gas that is sucked into the compressor, to the displacement volume of the piston

η^{ex}_{cycle} Exergetic efficiency of the refrigerating cycle

$coef_{area}$ Area coefficient of solar panels: ratio of the area of photovoltaic cells to the whole area of the panel

$coef_{rest}$ Mean restitution coefficient of electrical energy stored in electric batteries

$coef_{load}$ Coefficient of loading: ratio of cold utilized to cool the products within the refrigerating compartment to the total cold produced by the plant

$coef_{sec}$ Security coefficient: ratio of solar energy utilized to satisfy the total cooling needs of the apparatus to the total collected solar energy

$coef_{work}$ Coefficient of work of the motor: ratio of the duration of the working period of the electric motor to the total duration of working and non-working periods

$\bar{T}$ Mean temperature during the working period

$\bar{\bar{T}}$ Mean temperature during the total working and non-working period

h.t.c. Overall heat transfer coefficient (evaporator, condenser, refrigerating compartment)

S_{min} Minimal (optimum) area of collector needed under the conditions of use

γ Mean isentropic expansion coefficient of R 12 $\left(\gamma = \frac{c_p}{c_v}\right)$

ρ Quality factor of polytropic compression

m Mean polytropic expansion coefficient $\left(m = \frac{1-\rho}{\frac{1}{\gamma} - \rho}\right)$

References

1 D. I. Tchernev, *Proc. XIVth Intersoc. Energy Conversion Eng. Conf., Boston 1979*, American Chemical Society, Washington, DC, 1979, pp. 2070 - 2073.
F. Meunier, *cahier AFEDES*, No. 5, EETI, Paris, 1978.

2 A. Adell, *Rev. Gen. Froid*, Mai (1982).

3 H. Glaser, *Kaltetechnik, 15* (1963) 344 - 353.
W. Tripp, *ASHRAE J.*, (Jan.) (1966) 49 - 57.
ASHRAE Handbook of Fundmentals,, ASHRAE, New York, 1977.
H. Auracher, Saving of energy in refrigeration, International Institute of Refrigeration, IIF, Paris, 1980.

4 A. Adell, *Proc. XVIth Int. Refrigeration Congress, Paris, 1983*, IIF Commission B25, Paris, 1983, pp. 245 - 251.